Experimental Investigation of Control Strategies for an Asymmetric Cylinder with Two Individually Controlled Pumps

Samuel Kärnell[1], Axel Jemsson[1], Simon Johansson[1], and Liselott Ericson[1]

[1]Division of Fluid and Mechatronic Systems, Linköping University, Linköping, Sweden
E-mail: samuel.karnell@liu.se

Abstract

This paper investigates various control strategies for an electro-hydraulic actuator (EHA) equipped with two speed-controlled pumps, enabling simultaneous control of speed and pressure. The study examines the design and implementation of several control structures, including PI-controllers with feed-forward and different decoupling techniques, fuzzy logic controllers, optimal state feedback, and reinforcement learning. Initially, all control strategies were tested in a simulation environment, followed by validation in a laboratory test rig. The results demonstrate that even relatively simple control strategies can achieve satisfactory performance. Velocity feed-forward combined with a decoupled PI-controller for pressure showed strong performance and was easy to tune. Incorporation of fuzzy logic and virtual states could improve the performance further, but this came with additional efforts in design and tuning.

Keywords: Electro-hydraulic actuator, electrification, control

1 Introduction

As a way to reduce the CO2 emissions, the electrification of mobile machinery is ongoing. This provides incentives to improve energy efficiency as well as allowing for new system designs. Solutions with electro-hydraulic actuators (EHAs) are commonly discussed as a way forward. However, there are plenty of ways of realising EHAs, especially for asymmetrical cylinders since the differential flow can be handled in several ways. To get an idea of this, see [1]. This paper focuses on a concept that uses two individually controlled hydraulic units to take care of the differential flow. The layout of the concept and how it works in different modes of operation is illustrated in Fig. 1. As the figure shows, the hydraulic pumps can work in both pump and motor modes. However, for simplicity, from here on they will be referred to as pumps.

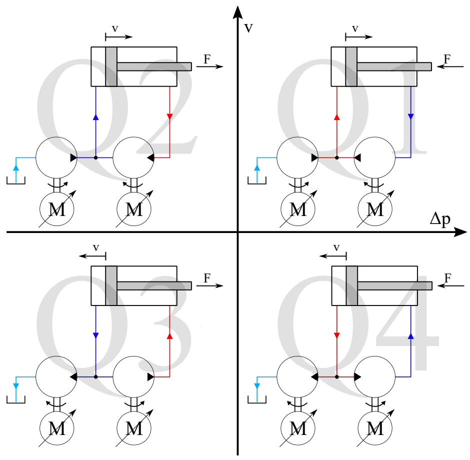

Figure 1: The concept studied in this paper and how it operates in different modes.

1.1 State of the art

A feature of the concept that is presented here is that it enables simultaneous pressure and speed (or position) control. However, the concept is not novel; a variant was patented in the early 90s [2]. At that time, it was proposed to have the pumps connected to the same shaft and to use the displacement setting for the control. The concept has regained attention in recent years, but now it is pumps with their own speed-controlled electric motors that are primarily getting attention.

The system is a multiple-input multiple-output (MIMO) system. The inputs are the signals to the electric motors (typically speed or torque) and the outputs are actuator speed (or position) and pressure (typically the low-pressure side of the actuator). Most work related to this concept is based on a specific kind of decoupled controller [3–6], but other simpler approaches have also been proposed [7]. Still, literature on practical implementation of controllers is limited even though examples can be found [8].

1.2 Contributions

In this paper, several control strategies are presented and evaluated in a physical test rig. The paper is based on the master's thesis by Jemsson and Johansson [9] and can be considered a condensed version.

2 System description

A detailed circuit diagram of the hydraulic system used for evaluation is shown in Fig. 2. The system was developed and built by Gnutti Carlo Sweden AB. Check valves and pressure relief valves are installed to prevent cavitation and overpressure. Electrically controlled load holding valves are implemented to unload the pumps when the cylinder is intended to be stationary. The pressure source shown in the figure was realised by an additional supply pump, providing about 5.5 bar.

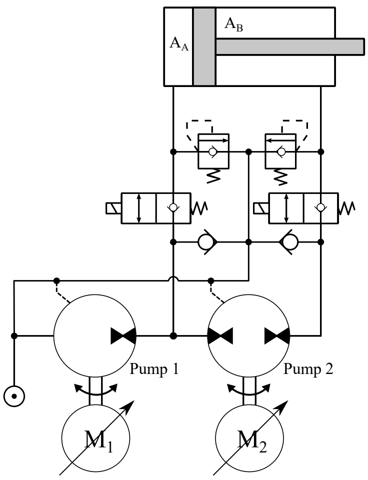

Figure 2: Detailed circuit diagram for the analysed system.

The circuit was implemented on the stick cylinder of an excavator arm in a lab environment. Weights were used as load. The pump and valve unit was placed on the side. The rig is shown in Fig. 3 and relevant system parameters are presented in Table 1.

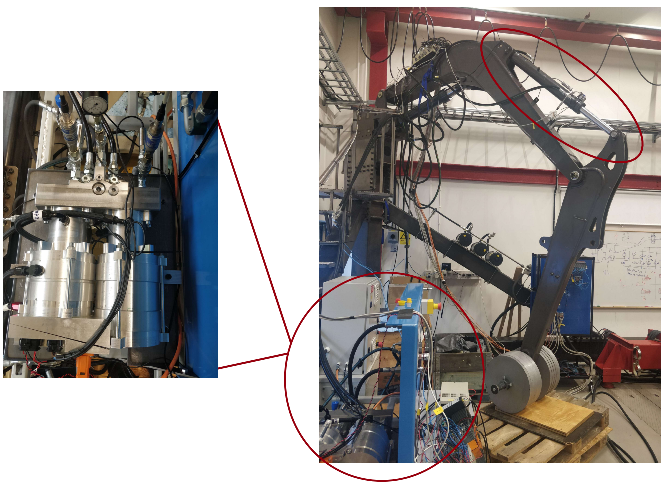

Figure 3: The test rig developed by Gnutti Carlo Sweden AB.

3 Modelling

A Simscape model of the system was created to allow for design, tuning, and testing of controllers before evaluation in the rig. Model parameters were adapted to measurement data. The model fit is exemplified in Fig. 4.

Table 1: System parameters.

	Symbol	Value	Unit
Cylinder stroke	$x_{\max}$	0.6	m
Cylinder linearization point	x_0	0.3	m
Cylinder area A side	A_A	0.0071	m^2
Cylinder area B side	A_B	0.0020	m^2
Hose volume A side	V_{Ah}	0.002	m^3
Hose volume B side	V_{Bh}	0.002	m^3
Displacement pump 1	D_1	14	cm^3/rev
Displacement pump 2	D_2	7	cm^3/rev
Tank pressure	p_t	5.5	bar
Maximum stroke	$x_{\max}$	0.6	m
Bulk modulus	β_e	1	MPa

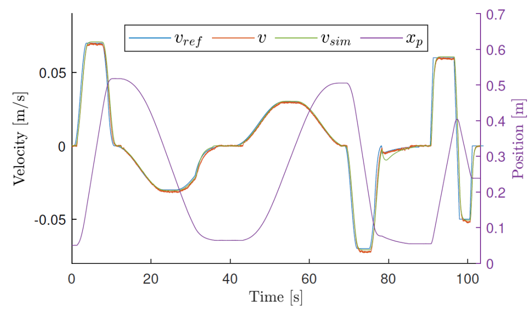

(a) Piston velocities.

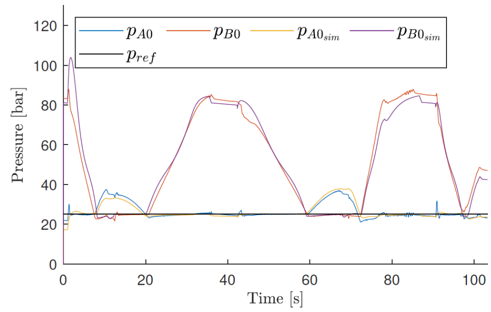

(b) Pressures measured at the cylinder.

Figure 4: Comparison of Simscape model and measurements.

In addition to the Simscape model, a linear model, which most of the controllers were based on, was formulated using the following equations:

$$m_{eq}\dot{v}_p = p_{A0}A_A - p_{B0}A_B - Bv_p - F, \tag{1}$$

$$\dot{p}_{A0} = \frac{\beta_e}{V_{A0}}\left(D_1 n_{p1} + D_2 n_{p2} - v_p A_A\right), \tag{2}$$

$$\dot{p}_{B0} = \frac{\beta_e}{V_{B0}}\left(-D_2 n_{p2} + v_p A_B\right). \tag{3}$$

p_A and p_B are the pressures on the A and B sides respectively, and index 0 represents a linearisation point. The equations above can be rewritten in state-space form as follows:

$$\dot{x}_M = A_M x_M + B_M u_M, \quad y_M = C_M x_M \tag{4}$$

where

$$x_M = \begin{bmatrix} v_p & p_{A0} & p_{B0} \end{bmatrix}^T, \quad u_M = \begin{bmatrix} n_{p1} & n_{p2} \end{bmatrix}^T,$$

$$A_M = \begin{bmatrix} -\frac{B}{m_{eq}} & \frac{A_A}{m_{eq}} & -\frac{A_B}{m_{eq}} \\ -\frac{A_A \beta_e}{V_A} & 0 & 0 \\ \frac{A_B \beta_e}{V_B} & 0 & 0 \end{bmatrix},$$

$$B_M = \begin{bmatrix} 0 & 0 \\ \frac{D_1 \beta_e}{V_A} & \frac{D_2 \beta_e}{V_A} \\ 0 & -\frac{D_2 \beta_e}{V_B} \end{bmatrix},$$

$$C_M = \begin{bmatrix} 1 & 0 & 0 \\ 0 & 1 & 0 \\ 0 & 0 & 1 \end{bmatrix}.$$

4 Control strategies

The following control strategies have been evaluated:

- PI-controller with feed-forward (section 4.1)
- Decoupled PI-controller with feed-forward (section 4.2)
- Fuzzy logic PI-controller with feed-forward (section 4.3)
- Decoupled PI-controller with virtual states (section 4.4)
- Linear-quadratic-integral control (section4.5)
- Linear-quadratic regulator with virtual states (section4.6)
- Feed-forward with reinforcement learning (section4.7)

All controllers aim to control cylinder speed and pressure on the low-pressure side. They will only be briefly described here. For a more comprehensive description of the controllers, see [9].

4.1 PI-controller with feed-forward

This can be considered the simplest controller of the ones presented in this paper. It utilises the relationships between pump speeds and cylinder velocity in the continuity equations **??** and **??**, neglecting pressure dynamics. The structure of the controller is shown in Fig. 5. In [7], it was shown that the first pump should be used to control the pressure when working in Q2 and Q3, whilst the second should be used when working in Q1 and Q4. However, that introduces a switch case which can cause oscillations. Therefore, the alternative to use the first pump to always control the pressure has also been investigated. Using the second pump has not been considered since that is more prone to instability in certain modes.

The pressure controller is a PI-controller, and the velocity controller is simply a gain of 1. The W-matrix is set to W_{M1} when

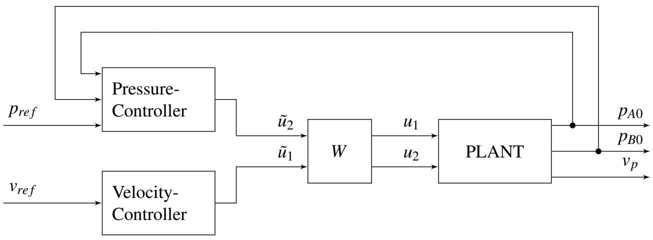

Figure 5: PI-controller with feed-forward.

p_{A0} is controlled and W_{M1} or W_{M2} when p_{B0} is controlled (depending on whether the first or second pump is used for the pressure control).

$$W_{M1} = \begin{bmatrix} \frac{A_A - A_B}{D_1} & 1 \\ \frac{A_B}{D_2} & 0 \end{bmatrix}, \quad W_{M2} = \begin{bmatrix} \frac{A_A - A_B}{D_1} & 0 \\ \frac{A_B}{D_2} & -1 \end{bmatrix}.$$

4.2 Decoupled PI-controller with feed-forward

In contrast to the controller described in Section 4.1, this controller partially decouples the pressure from the velocity by utilising the pressure build-up in the continuity equations. This has an impact on the W-matrix, which now depends on the volumes and is therefore updated based on the cylinder position. The W-matrix becomes as follows:

$$W = \begin{bmatrix} \frac{A_A - A_B}{D_1} & \frac{\frac{A_B}{A_A} V_A + V_B}{\beta_e D_1} \\ \frac{A_B}{D_2} & -\frac{V_B}{\beta_e D_2} \end{bmatrix}.$$

The structure of the controller is shown in Fig. 6.

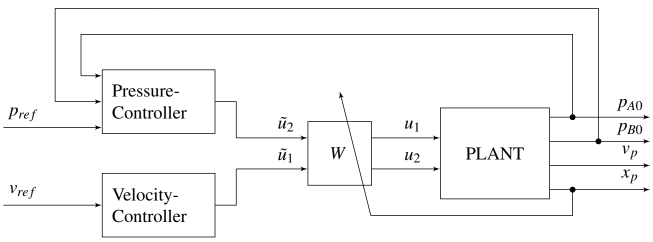

Figure 6: Decoupled PI-controller.

4.3 Fuzzy logic PI-controller with feed-forward

This controller is an extension of the decoupled PI-controller presented in Section 4.2. It uses so-called fuzzy logic to adjust the gains of the PI-controller. The core of the fuzzy logic lies in the rule table, which specifies how the output should be based on the input. In this case, the pressure error (e) and the derivative of the error (de) are inputs (called fuzzy variables). The rule table developed for the fuzzy logic is shown in Table 2. **Z** represents zero, **VS** represents very small, **S** represents small, **M** represents medium, and **B** represents big. Based on these different error inputs, the rule table determines the output values for both the proportional gain and the integral gain. These output values are also abbreviated, where **VS** means very small, **S** means small, **M** means medium, **B** means big, and **VB** means very big. For information on how the outputs from the table are translated into controller gains, see [9].

$\lvert e\rvert\backslash\lvert de\rvert$	Z	VS	S	M	B
Z	(S,VB)	(S,VB)	(VS,VB)	(VS,VB)	(VS,VB)
VS	(S,VB)	(S,VB)	(S,VB)	(VS,B)	(VS,B)
S	(M,B)	(M,B)	(M,B)	(S,M)	(S,M)
M	(B,VS)	(B,VS)	(B,S)	(M,S)	(M,S)
B	(VB,S)	(VB,S)	(VB,S)	(VB,S)	(B,S)

Table 2: Rule table.

The structure of the controller is shown in Fig. 7.

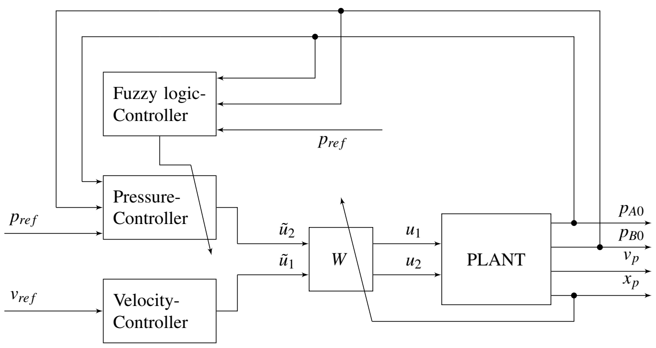

Figure 7: Decoupled fuzzy PI-controller.

4.4 Decoupled PI-controller with virtual states

This controller is based on the one presented in [3]. It utilises virtual states to facilitate full decoupling. The structure of the controller is shown in Fig. 8.

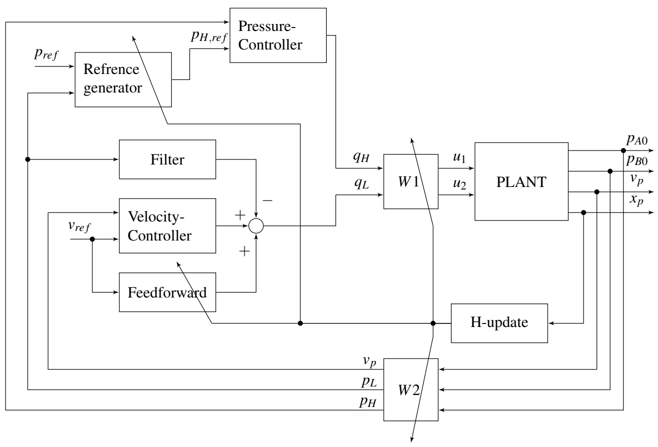

Figure 8: Decoupled controller with virtual states.

The W-matrices are:

$$W_1 = \begin{bmatrix} D_1 & D_2\left(1+\frac{1}{H}\right) \\ D_1 & D_2\left(1-\frac{1}{\alpha}\right) \end{bmatrix}^{-1}, \quad W_2 = \begin{bmatrix} 1 & 0 & 0 \\ 0 & 1 & -\alpha \\ 0 & 1 & H \end{bmatrix},$$

where $H = \rho/\alpha$, $\rho = V_B/V_A$ and $\alpha = A_B/A_A$.

4.5 Linear-quadratic-integral control

Modern control often relies on optimal state feedback controllers, with the linear-quadratic regulator being a commonly used example. Here, two variants were implemented and evaluated. One of them was based on so-called linear-quadratic-integral control (LQI), in which the error is integrated. Its structure is shown in Fig. 9.

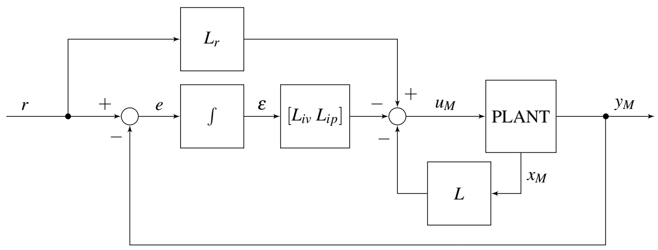

Figure 9: LQI controller.

4.6 Linear-quadratic regulator with virtual states

The other optimal state feedback controller that was tested was a linear-quadratic regulator (LQR) that utilises virtual states, inspired by the controller presented in Section 4.4. This to account for disturbances. It is shown in Fig. 10.

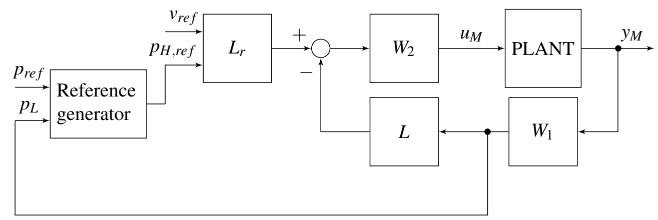

Figure 10: LQR controller.

4.7 Feed-forward with reinforcement learning

The last controller to be evaluated was based on reinforcement learning (RL) together with feed-forward. Its structure is shown in Fig. 11. The reinforcement used the so-called twin-delayed deep deterministic (TD3) policy gradient algorithm. It was trained on the Simscape model. The feed-forward was the same as in the PI-controller presented in section 4.1.

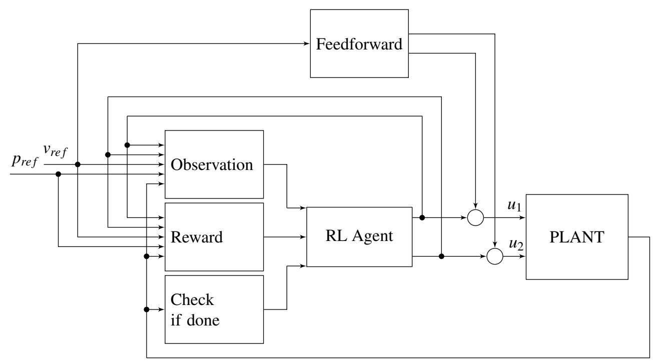

Figure 11: RL-based controller.

5 Results

The different control strategies were evaluated in the test rig described in section 2 using a drive cycle that forces the EHA to work in all four modes of operation. Results for the controllers described above are presented below in Fig. 12 to 19.

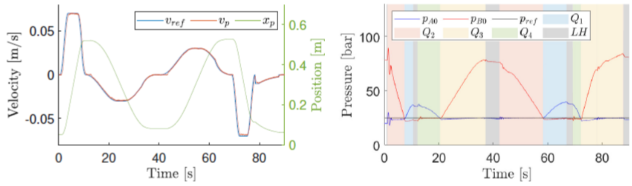

Figure 12: PI-controller (using pump 1 for pressure control).

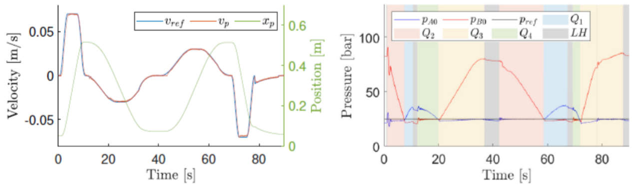

Figure 13: PI-controller.

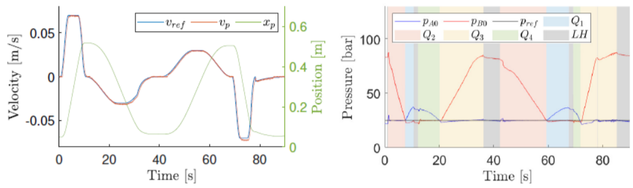

Figure 14: Decoupled PI-controller.

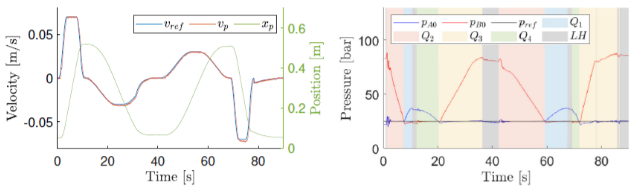

Figure 15: Decoupled fuzzy logic PI-controller.

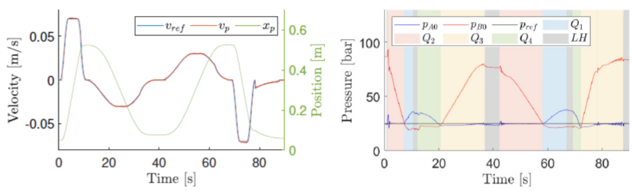

Figure 16: Decoupled PI-controller with virtual states.

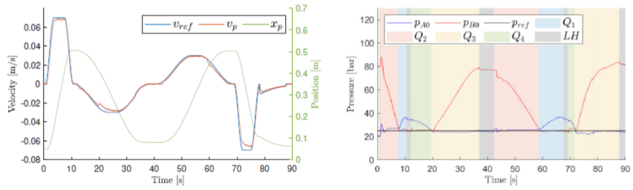

Figure 17: LQI controller.

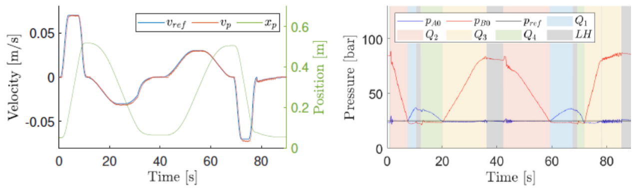

Figure 18: LQR controller with virtual states.

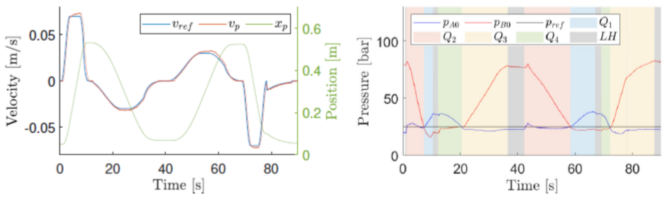

Figure 19: Reinforcement learning-based controller.

It can be seen that all controllers perform quite similarly. They manage to track the velocity and pressure fairly well. To better show how they differ, the root mean square error (RMSE) for the velocity and pressure is presented in Table 3. It also shows the RMSE values for a step response (again, see [9] for details). In addition, a somewhat subjective measure of "tuneability" is included, where "A" is easy and "F" is difficult.

	PI (M1)	**PI**	**Dec.**	**Fuz.**	**Vrt. st.**	**LQI**	**LQR**	**RL**
V. [mm/s]	3.1	2.7	3.2	3.2	2.1	3.3	3.2	4.1
P. [bar]	1.22	1.53	1.04	0.85	2.19	1.20	1.12	2.86
V. step [mm/s]	9.9	9.7	9.5	9.6	7.3	9.9	9.5	12.0
P. step [bar]	7.48	8.95	1.41	1.20	1.49	2.79	1.32	3.48
Tuneability	B	B	A	D	D	D	C	F

Table 3: RMSE values for different controllers. The three best controllers in each category are colour-coded, where gold is the best, silver is second, and bronze is third.

When examining the table, it can be noted that the controller using virtual states has the best velocity tracking, and that the fuzzy logic has best pressure tracking. However, they are considered to require considerably higher tuning effort than e.g. the decoupled PI-controller, which in fact performs quite similar. Even the simple feed-forward controllers perform somewhat well, with the exception of the pressure control during the step response.

6 Discussion

Satisfactory results were achieved with all controllers. This means that the simpler controllers can likely be considered good enough in many applications. However, the electric motors that were used in the test rig had slow dynamics. For faster systems, it is likely that larger differences would emerge. It should also be mentioned that the result do not say too much about the full potential of the controllers since the tuning was performed manually. Nonetheless, it gives an insight into the level of performance achievable with reasonable tuning and modelling effort.

Furthermore, an advantage of the simpler controllers is their predictability. It is easy to understand what they are doing and why. This makes them more pleasant to run in the rig from an operability point of view.

Another thing to note is that all controllers, except the simplest feed-forward controller, relied on position and/or velocity feedback. Eliminating the need for such feedback can be considered an advantage since fewer sensors are required.

7 Conclusions

Feed-forward with a decoupled PI-controller can achieve good performance with low effort. Better performance can be achieved by using fuzzy logic to set the controller gains, but at the cost of increased controller complexity and tuning effort. Similarly, decoupling using virtual states also improves performance but requires additional tuning.

Acknowledgements

This research was funded by the Swedish Energy Agency (Energimyndigheten) with grant number P2023-00594. Gnutti Carlo Sweden AB have supported with hardware for the rig.

References

[1] Søren Ketelsen, Damiano Padovani, Torben O Andersen, Morten Kjeld Ebbesen, and Lasse Schmidt. Classification and review of pump-controlled differential cylinder drives. *Energies*, 12(7):1293, 2019.

[2] Jorg Dantlgraber. Hydraulic system for a differential piston type cylinder, January 19 1993. US Patent 5,179,836.

[3] Søren Ketelsen, Torben Ole Andersen, Morten Kjeld Ebbesen, and Lasse Schmidt. A self-contained cylinder drive with indirectly controlled hydraulic lock. *Modeling, Identification and Control*, 41(3):185–205, October 2020.

[4] Viktor Donkov, Søren Ketelsen, Torben Andersen, Morten Kjeld Ebbesen, and Lasse Schmidt. Improving the performance of self-contained cylinder drives with load-holding capabilities. In *Scandinavian International Conference on Fluid Power (SICFP21)*, pages 50–61, 2021.

[5] Wei Zhao, Mohit Bhola, Morten K Ebbesen, and Torben Ole Andersen. A novel control design for realizing passive load-holding function on a two-motor-two-pump motor-controlled hydraulic cylinder. *Modelling, Identification, and Control*, 44(3):125–139, 2023.

[6] Wei Zhao, Mohit Bhola, Morten Kjeld Ebbesen, and Torben Ole Andersen. A motor-controlled hydraulic cylinder with cylinder pressure control and load-holding function-an experimental study. In *Fluid Power Systems Technology*, volume 87431.

[7] Samuel Kärnell and Liselott Ericson. Control of an asymmetric cylinder with two individually controlled pump/motors. volume ASME/BATH 2023 Symposium on Fluid Power and Motion Control of *Fluid Power Systems Technology*.

[8] Wei Zhao, Morten Kjeld Ebbesen, Michael Rygaard Hansen, and Torben Ole Andersen. Experimental assessment of energy consumption: a comparative study between motor-controlled and valve-controlled cylinders in knuckle boom crane operations. *Frontiers in Mechanical Engineering*, 11, 2025.

[9] Simon Johansson and Axel Jemsson. Investigation of control strategies for an electro-hydraulic actuator with dual variable-speed pumps: An applied study on an excavator arm with load-holding capabilities. Master's thesis, Linköping University, 2024. LIU-IEI-TEK-A–24/04784–SE.